Thermochimica Acta 510 (2010) 202–212

Contents lists available at ScienceDirect

Thermochimica Acta

journal homepage: www.elsevier.com/locate/tca

Experimental investigations and thermodynamic description of the $PbO–Fe_2O_3$ system

I. Diop, N. David*, J.M. Fiorani, R. Podor, M. Vilasi

Laboratoire de Chimie du Solide Minéral - UMR 7555, Université Henri Poincaré, Nancy 1, Bd des Aiguillettes, F-54506 Vandœuvre-lès-Nancy, France

ARTICLE INFO

Article history:
Received 4 March 2010
Received in revised form 6 July 2010
Accepted 13 July 2010
Available online 23 July 2010

Keywords:
T91
Spallation target
$PbO–Fe_2O_3$
Phase diagram
Thermodynamic assessment

ABSTRACT

The knowledge of the quinary Pb–Bi–O–Fe–Hg is necessary for understanding the degradation mechanisms of the T91 steel used as structure material in future ADS nuclear reactors. In this device, the steel will be in direct contact with the liquid spallation target (which is constituted by lead or lead-bismuth eutectic) surrounded by a reduced oxygen pressure atmosphere. In the present work, the characterization of the pseudo-binary $PbO–Fe_2O_3$ cut has been performed. In order to complete the available data in the literature, some experimental investigations by differential thermal analysis (DTA), isothermal annealing, powder X-ray diffraction analysis (XRD), scanning electron microscopy (SEM) and electron probe microanalysis (EPMA) have been done. These results have allowed proposing a thermodynamic assessment using the Calphad method.

1. Introduction

The T91 steel (9%Cr–1%Mo) is considered as structural material in the new generation of nuclear reactors named ADS (Accelerator Driven System). In this device, the steel will be in direct contact with the liquid spallation target (which is constituted by lead or lead-bismuth eutectic, 55.2 wt% Bi). It is necessary to evaluate the corrosion resistance of the T91 steel in an eutectic liquid lead-bismuth environment, under a low oxygen pressure, more particularly in the temperature range 350–600 °C. The first immersion tests have shown that complex oxides of Fe, Bi and Pb were formed [1] leading to the conclusion that a complete thermodynamic assessment of the quinary Pb–Bi–O–Fe–Hg system would be useful for understanding and interpreting the corrosion results.

In order to model the quinary system, it is necessary in a first step to complete the modeling of the ternary sub-systems. The study of some of them (Pb–Bi–Hg and Bi–Fe–O) has been initiated experimentally in our laboratory [2–4]. In the present work, the efforts were focused on the ternary Pb–Fe–O and more particularly on the investigation on the pseudo-binary $PbO–Fe_2O_3$ cut.

2. Review of the experimental data

Several studies conducted by different authors have allowed knowing the phase diagram. But if the existence of intermediate phases has been put in evidence there are still some disagreements about their formulae, homogeneity ranges, stability temperature ranges and crystallographic structures.

One of the first important studies on the $PbO–Fe_2O_3$ system is due to Cocco in 1955 [5]. By using X-ray diffraction analysis and optical microscopy, he has succeeded in determining the stoichiometry of the compounds formed with PbO and Fe_2O_3 powders mixture: $Pb_2Fe_2O_5$(2:1), $Pb_2Fe_{10}O_{17}$(2:5) and $PbFe_{10}O_{16}$(1:5). An eutectic reaction $L \rightarrow PbO + Pb_2Fe_2O_5$(2:1) is reported at 730 °C and at 11 mol.% Fe_2O_3. Then Berger and Pawlek [6] in 1957 have synthesized $Pb_2Fe_2O_5$(2:1), $PbFe_4O_7$(1:2) and $PbFe_{12}O_{19}$(1:6). Margulis and Kopylov [7] in 1960 have identified by XRD only one compound, $PbFe_8O_{13}$(1:4), which peritectoïd temperature of formation would be equal to 1140 °C. Moreover, they have founded the eutectic invariant reaction at 720 °C and at 12.5 mol.% of Fe_2O_3. A detailed study of alloys containing 34 to 87 mol.% Fe_2O_3 is carried out by Mountvala and Ravitz [8] in 1962 by using XRD and differential thermal analysis techniques. The authors have verified the existence of three phases named δ, γ and β. The δ-phase corresponds to the $Pb_2Fe_2O_5$(2:1) compound identified by Cocco and β-phase corresponds to $PbFe_{12}O_{19}$(1:6) compound identified by Berger and Pawlek. According to Mountvala and Ravitz, the two γ and β phases are extending from $PbFe_4O_7$(1:2) to $Pb_2Fe_{10}O_{17}$(2:5) and from $PbFe_{10}O_{16}$(1:5) to $PbFe_{12}O_{19}$(1:6) respectively. The three phases are formed by peritectic reactions which occur at 910 °C (δ),

* Corresponding author.
E-mail addresses: ibra.diop@lcsm.uhp-nancy.fr (I. Diop), nicolas.david@lcsm.uhp-nancy.fr (N. David), jean-marc.fiorani@lcsm.uhp-nancy.fr (J.M. Fiorani), renaud.podor@lcsm.uhp-nancy.fr (R. Podor), michel.vilasi@lcsm.uhp-nancy.fr (M. Vilasi).

0040-6031/$ – see front matter © 2010 Elsevier B.V. All rights reserved.
doi:10.1016/j.tca.2010.07.015

945 °C (γ) and 1315 °C (β), respectively. The eutectoid decomposition temperatures of the δ-$Pb_2Fe_2O_5$(2:1), γ and β-$PbFe_{12}O_{19}$(1:6) compounds are determined equal to 650 °C, 750 °C and 760 °C respectively. The composition of the eutectic liquid between PbO and δ-$Pb_2Fe_2O_5$(2:1) corresponds to 18 mol.% of Fe_2O_3.

At the same time, Chizhikov and Konvshkova in 1963 [9] and Rudnichenko and Dobrotsevtov in 1965 [10] have confirmed the work of Mountvala and Ravitz. The first team has detected two compounds $PbFe_2O_4$(1:1), $Pb_2Fe_{10}O_{17}$(2:5) and the eutectic reaction. The last mentioned researchers have observed the formation of δ-$Pb_2Fe_2O_5$(2:1) and $PbFe_2O_4$(1:1). Later in 1975, studying on a complex system composed by boron, lead, iron and yttrium oxides, Jonker [11] has produced data about liquidus points of PbO–Fe_2O_3 system.

More recently, some other authors have confirmed or disproved these results. In 1978, Mexmain and Hivert [12] have first studied the influence of the powder milling and researched the limit temperature from which the volatilization of PbO is not negligible (800 °C). After that, they have identified the $PbFe_4O_7$(1:2), $PbFe_6O_{10}$(1:3) and β-$PbFe_{12}O_{19}$(1:6) phases and determined the value of the eutectic liquid composition (14 mol.% of Fe_2O_3) which is in non-agreement to that proposed by Mountvala and Ravitz (18 mol.% of Fe_2O_3). The eutectic temperature is located at 780 °C. The temperature of the peritectic reaction L + $PbFe_6O_{10}$(1:3) → δ-$Pb_2Fe_2O_5$(2:1) and L + β-$PbFe_{12}O_{19}$(1:6) → $PbFe_6O_{10}$(1:3) are notified at 877 °C and 911 °C respectively.

Shaaban et al. [13] in 1984 have investigated the ternary Pb–Fe–O system below 700 °C taking into account the possible valences of Pb and Fe and more particularly the PbO_2-Fe_2O_3 isopleth cut which corresponds to the highest lead valency (IV). In this case they have found that it is possible to form the (2:1) compound and the γ-phase at lower temperatures (410 °C and 430 °C respectively) than in the PbO–Fe_2O_3 isopleth cut (650 °C and 750 °C respectively). According to Shaaban et al. [13], the non-stoichiometry range of the β solid solution corresponds to PbO–(4-6)Fe_2O_3. Moreover, they have indicated a solubility of Fe_2O_3 in PbO extending to about 6% Fe_2O_3. Nevriva and Fischer [14] in 1986 and Rivolier et al. [15] in 1993 have reported the existence of the δ-$Pb_2Fe_2O_5$(2:1), $Pb_2Fe_{10}O_{17}$(2:5) and β-$PbFe_{12}O_{19}$(1:6) compounds. Rivolier et al. [15] have studied the phase equilibria under an oxygen pressure equal to 1 atm. Above 1200 °C, they evidenced the difficulty of performing experiments, the decomposition of β-$PbFe_{12}O_{19}$(1:6) involving solid-liquid-vapor equilibria in the ternary PbO–FeO–O_2 system. The results of DTA obtained by [14] and [15] led to the same composition of the eutectic liquid at 11 mol.% of Fe_2O_3 and confirmed Cocco value [5]. Moreover Nevriva and Fischer have indicated the non-stoichiometry of $PbFe_4O_7$(1:2), which is mentioned first by Mountvala and Ravitz. Nevriva and Fischer [14] have measured the L → PbO + δ-$Pb_2Fe_2O_5$(2:1) invariant reaction at 760 ± 5 °C, the L + $PbFe_4O_7$(1:2) → δ-$Pb_2Fe_2O_5$(2:1) reaction at 870 ± 5 °C and the L + β-$PbFe_{12}O_{19}$(1:6) → $PbFe_4O_7$(1:2) reaction at 880 ± 5 °C. For the same equilibria, Rivolier et al. [15] have determined the invariant temperatures at 780 ± 2 °C, 870 ± 10 °C and 915 ± 10 °C respectively. The liquidus temperatures measured by Rivolier et al. in the two-phase domains L + β-$PbFe_{12}O_{19}$(1:6), L + $Pb_2Fe_{10}O_{17}$(2:5) and L + δ-$Pb_2Fe_2O_5$(2:1) are in good agreement with those obtained by Jonker [11] and by Nevriva and Fischer [14], notably at high temperature. Otherwise no Fe_2O_3 solubility in PbO is found by Rivolier et al. [15], neither by Mountvala and Ravitz [8] nor by Nevriva and Fischer [14], contrarily to Shaaban et al. [13].

In all the previous studies the different authors have used the X-ray diffractometry to identify the synthesized compounds. Their contributions have conducted to the establishment of ASTM files compiled in the JCPDS database [16]. A carefully consultation of this database reveals the existence of three different files corresponding to the three $PbFe_4O_7$(1:2), $PbFe_6O_{10}$(1:3) and $Pb_2Fe_{10}O_{17}$(2:5) compounds. But an attentive examination of them exhibits the same X-ray powder diffraction pattern for the three phases. Indeed, the compounds are characterized by the same hexagonal structure and quite the same parameters: a = 5.9 Å and c = 23.5 Å. Concerning the latter, one can notice that its value varies from 23.0 to 23.8 Å depending on the considered study. Therefore, the respective d_{hkl} are practically identical. This fact suggests the non-stoichiometry of the intermediate compounds named γ by Mountvala and Ravitz [8]. In the following of this study the γ phase will be noted γ-

Table 1
Crystallographic data on the PbO–Fe_2O_3 system.

Phase	Composition (mol.% Fe_2O_3)	Space Group
PbO-L (T < 762 K)	0	P4/nmm
PbO-M (T > 762 K)	0	Pbma
δ-$Pb_2Fe_2O_5$(2:1)	32.5	C
γ-$Pb_2Fe_{10}O_{17}$(2:5)	71–75	P312
β-$PbFe_{12}O_{19}$(1:6)	84.5	$P6_3/mmc$
Fe_2O_3	100	$R\bar{3}c$

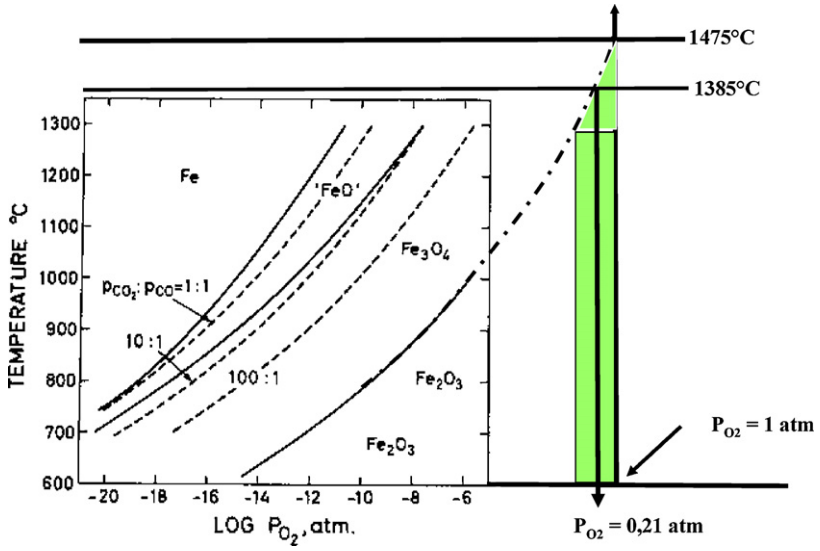

Fig. 1. Stability of Fe_2O_3 versus temperature [17].

$Pb_2Fe_{10}O_{17}$(2:5). The crystal structures of the retained phases are summarized in Table 1.

In the present work we propose to reinvestigate all compositions and temperature ranges of the PbO–Fe_2O_3 system in order to obtain the most coherent diagrammatic information which is essential for performing the Calphad modeling.

3. Procedure and materials

3.1. Differential thermal analysis

The samples are prepared at room temperature and in air under atmospheric pressure in an agate mortar by mixing the oxide powders provided by Chempur (PbO (litharge), 99.999% and Fe_2O_3, 99.9%). Several samples of each investigated composition are prepared in order to carry out DTA experiments and annealings at different temperatures. The effect of the oxygen partial pressure is studied by employing two different ways: (i) the static air atmosphere having a total pressure equal to 1 bar and (ii) a dynamic argon atmosphere in which the oxygen impurity fixes the reduced oxygen pressure (value of PO_2 < 2 ppm wt.%).

(i) The mixture of powders is introduced into platinum crucibles who are sealed by electrical arc in order to limit the lead oxide lost by vaporization at high temperature. In this configuration, the volume of air contained in the crucible above the sample at room temperature can be estimated to be equal to 0.4 cm^3. At the highest temperature reached during the experiment (1400 °C), Fe_2O_3 is stable (Fig. 1) and the oxygen partial pressure becomes equal to 1 atm. The results of theses experiments are comparable to those obtained by Rivolier et al. [15] who worked under PO_2 = 1 atm. We can note that under atmospheric conditions, the maximal temperature of Fe_2O_3 stability is close to 1385 °C [17].

(ii) In order to fix a reduced pressure of oxygen, a mixture of powder is introduced in a platinum crucible kept open during the measure. A DTA starting from room temperature to 1300 °C with a heating rate of 5 °C/min is carried out under argon. The result of this experiment shows that the lead oxide is reduced leading to the formation of low melting point compounds with platinum and lead (Fig. 2). Therefore, the powders of lead oxide and iron oxide are placed in an alumina crucible. A first treatment is applied to the powders in order to alloyed pure oxides. This step consists in an annealing characterized by a heating rate of 5 °C/min starting from room temperature until a high temperature which depends to the composition of the melt. Then the composition and the mass of each as-obtained sample are controlled. Transitions and melting points are determined by differential thermal analysis with a SETARAM DTA/TGA-92, a SETARAM DSC-111 and a SCERES microcalorimeter. These latter experiments are carried out with heating or cooling rates of 5 °C/min.

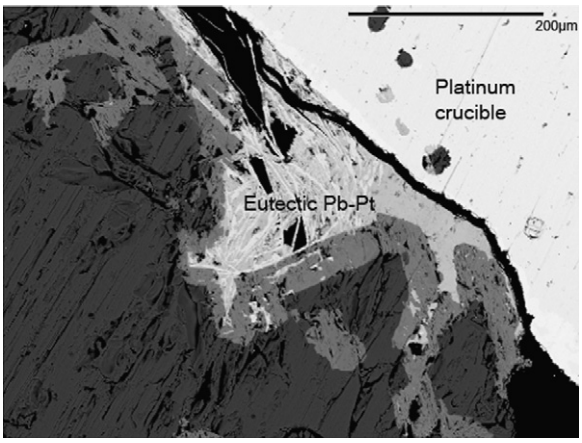

Fig. 2. Open platinum crucible deteriorated by reaction with lead (55 mol.% Fe_2O_3 sample).

3.2. Isothermal annealing

For this type of experiments, after having crushed the two pure oxide powders in an agate mortar, the mixture is pressed to form disks of 5 mm diameter and 3 to 5 mm thick. The as-obtained disks are weighted and placed inside furnaces. Two kinds of crucibles are used according to the temperature of annealing: alumina covered by BN for T > 1200 °C and gold for T < 1200 °C. The time of annealing varied from 2 hours to one month depending on composition and

Table 2
Gibbs energy of pure elements for stable and metastable phases taken from [18] database.

Element	Phase	T (K)	${}^0G_i^{\varphi}(T) - {}^0H_i^{\Phi}$ (298.15 K) (J/mol of atoms)
Pb	(Pb) (fcc-A1) GHSERPB	298.15–600.650	$+7650.085 + 101.715188\,T - 24.5242231\,T\ln T - 0.00365895\,T^2 - 2.4395\times10^{-07}\,T^3$
		600.650–1200	$-10{,}531.115 + 154.258155\,T - 32.4913959\,T\ln T + 0.00154613\,T^2 + 8.05644\times10^{25}\,T^{-9}$
		1200–5000	$+4157.596 + 53.154045\,T - 18.9640637\,T\ln T - 0.002882943\,T^2 + 9.8144\times10^{-08}\,T^3 - 2{,}696{,}755\,T^{-1} + 8.05644\times10^{25}\,T^{-9}$
O	Gas	298.15–1000	$+6961.74451 - 51.0057202\,T - 22.2710136\,T\ln T - 0.0101977469\,T^2 + 1.32369208\times10^{-06}\,T^3 - 76{,}729.7484\,T^{-1} + RT\ln P$
		1000–3300	$-13{,}137.5203 + 25.3200332\,T - 33.627603\,T\ln T - 0.00119159274\,T^2 + 1.35611111\times10^{-08}\,T^3 + 525{,}809.556\,T^{-1} + RT\ln P$
		3300–6000	$-27{,}973.4908 + 62.5195726\,T - 37.9072074\,T\ln T - 0.000850483772\,T^2 + 2.14409777\times10^{-08}\,T^3 + 8766421.4\,T^{-1} + RT\ln P$
O	GHSEROO	298.15–1000	$-3480.87 - 25.503038\,T - 11.136\,T\ln(T) - 0.005098888\,T^2 + 6.61846\times10^{-7}\,T^3 - 38{,}365\,T^{-1}$
		1000–3300	$-6568.763 + 12.65988\,T - 16.8138\,T\ln(T) - 5.95798\times10^{-4}\,T^2 + 6.781\times10^{-9}\,T^3 + 262{,}905\,T^{-1}$
		3300–6000	$-13{,}986.728 + 31.259625\,T - 18.9536\,T\ln(T) - 4.25243\times10^{-4}\,T^2 + 1.0721\times10^{-8}\,T^3 + 4{,}383{,}200\,T^{-1}$
Fe	(αFe,δFe) (bcc-A2)	298.15–1811	$+1224.83 + 124.134\,T - 23.5143\,T\ln T - 0.00439752\,T^2 - 5.89269\times10^{-08}\,T^3 + 77{,}358.5\,T^{-1}$
		1811–6000	$-25{,}384.451 + 299.31255\,T - 46\,T\ln T + 2.2960305\times10^{31+}\,T^{-9}$
	(γFe) (fcc-A1) GHSERFE	298.15–1811	$-1462.4 + 8.282\,T - 1.15\,T\ln T + 6.4\times10^{-04}\,T^2 + 1224.83 + 124.134\,T - 23.5143\,T\ln T - 0.00439752\,T^2 - 5.89269\times10^{-08}\,T^3 + 77{,}358.5\,T^{-1}$
		1811–6000	$-27{,}098.266 + 300.25256\,T - 46\,T\ln T + 2.78854\times10^{31+}\,T^{-9}$

Table 3a
Phases observed by SEM and EPMA (Simplified notation: x:$y = x$PbO–yFe$_2$O$_3$).

Compositions (mol.% Fe_2O_3)	Annealing temperatures (°C)	Observed phases	Compositions of phases (mol.% Fe_2O_3)	
10	800	Liquid + PbO	12.8	0
18	300, 400, 500	PbO + Fe_2O_3	0	100
19	713	PbO + (2:1)	0	32.38
25	800	(2:1) + Liquid	32.52	17.41
40	920	(1:6) + Liquid	84.54	21.2
50	910	(1:6) + Liquid	82.95	20.2
55	300, 400, 500	PbO + Fe_2O_3	0	100
40, 50, 60	1030	Liquid + (1:6)	19.55	84.42
68	665	Fe_2O_3 + (2:1)	100	31.59
58, 50, 67	700	Fe_2O_3 + (2:1)	100	32.50
68	875	Liquid + (2:5)	18.18	71.23
79	875	PF_6 + (2:5)	84.56	74.49
79	915	(1:6) + Liquid	85.6	20.15
80	920	(1:6) + Liquid	84.89	20.13
85	300, 400, 500	PbO + Fe_2O_3	0	100
90	920,1030	Fe_2O_3 + (1:6)	100	85.59

Table 3b
Analyze average realized starting from 20 measurements with EPMA.

	δ-$Pb_2Fe_2O_5$(2:1)	γ-$Pb_2Fe_{10}O_{17}$(2:5)	β-$PbFe_{12}O_{19}$(1:6)
Mol.% Fe_2O_3	32.44	71–75	84.50

temperature. The samples are quenched in air or in water when air quenching is not efficient.

After all experiments (DTA or isothermal annealing), the samples are analysed by EMPA (CAMECA SX 100), XRD (Philips X'pert Pro) and observed by SEM (Hitachi S-2500 and Philips XL 30).

4. Thermodynamic models

4.1. Gibbs energy for pure components

The Gibbs energy of formation noted GHSERi of a constituent i is described from a reference state generally chosen as the Φ stable state of the considered element at 298.15K under a pressure of 1 bar. The standard formation enthalpy of the reference state is function of temperature and is arbitrarily fixed equal to 0 at 298.15 K and is noted ${}^0H_i^{\Phi}$ (298.15 K). The Gibbs energy of formation of a constituent i is expressed by

$$ {}^0G_i^{\varphi}(T) - {}^0H_i^{\Phi}(298.15\,\mathrm{K}) = a + bT + cT\ln T + dT^2 + eT^{-1} + fT^3 + iT^7 + jT^{-9} \quad (1) $$

where ${}^0G_i^{\varphi}(T)$ is the molar Gibbs energy of the pure element i in the physical state φ at temperature T. The additional terms taking into account the effect of pressure of magnetism are considered because their contributions are not negligible in the present work. The thermodynamic functions of pure elements for stable and metastable phases taken from SGTE database by Dinsdale [18] are reported in Table 2.

4.2. Solid phases

The Gibbs energies of the oxides (PbO-Litharge, PbO-Massicot, δ-$Pb_2Fe_2O_5$(2:1), γ-$Pb_2Fe_{10}O_{17}$(2:5), β-$PbFe_{12}O_{19}$(1:6), and Fe_2O_3,) are described by the way of the sublattice model which has been developed by Sundman and Ågren [19]. Their work was based on earlier models, principally on the ionic model due to Temkin [20] and the two-sublattice model due to Hillert et al. [21]. According to this model, the different species forming the phase occupy one or more sublattices and thermodynamic quantities are expressed as a function of the site fractions. In this model a two-sublattice binary phase with concentration dependence is written as:

$$ (A_{y'_A}B_{y'_B})_p(A_{y''_A}B_{y''_B})_q $$

where y'_A, y'_B, y''_A and y''_B are respectively the fractional site occupation of each component A and B on the first and second sublattices and where p and q are the number of sites of each sublattice. The molar Gibbs energy of this phase is given by

$$ G_m^{\varphi} = y'_A y''_A {}^0G^{\varphi}_{A:A} + y'_A y''_B {}^0G^{\varphi}_{A:B} + y'_B y''_A {}^0G^{\varphi}_{B:A} + y'_B y''_B {}^0G^{\varphi}_{B:B} + PRT(y'_A \ln y'_A + y'_B \ln y'_B) + QRT(y''_A \ln y''_A + y''_B \ln y''_B) + {}^{Ex}G_m^{\varphi} $$

4.2.1. Stoichiometric compounds

In the PbO–Fe_2O_3 system, all intermediate phases are considered as stoichiometric compounds: δ-$Pb_2Fe_2O_5$(2:1), γ-$Pb_2Fe_{10}O_{17}$(2:5), β-$PbFe_{12}O_{19}$(1:6). The molar Gibbs energy is

Table 4
Experimental invariant equilibrium temperatures obtained by DTA (Simplified notation: x:$y = x$PbO–yFe$_2$O$_3$).

Invariant equilibria	Mol.% Fe_2O_3									
	27.5	30	35	50	55	67	68	70	80	85
(2:1) → PbO + Fe_2O_3	770		700	695	695	700	690	705	705	695
L → PbO + (2:1)		780								
(2:5) → (2:1) + Fe_2O_3			780	780	770		780	780		
(1:6) → (2:5) + Fe_2O_3									< 810	
L + (2:5) → (2:1)		860		850	850	860		860		
L + (1:6) → (2:5)	915			920	900					
L + Fe_2O_3 → (1:6)				1270	1315	1350		1350	1260	1270

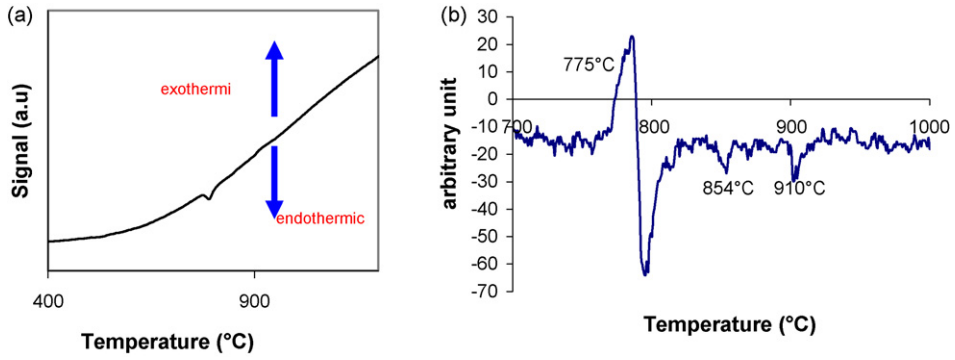

Fig. 3. Thermogram mixture PbO–Fe_2O_3 (27.5 mol.% Fe_2O_3).

expressed relative to ${}^0G^{Fe_2O_3}_{Fe_2O_3}$ and ${}^0G^{PbO-L}_{PbO}$ as follows

$$ {}^0G_m^{Fe_xPb_zO_{3x/2+z}} = \frac{x}{2}{}^0G^{Fe_2O_3}_{Fe_2O_3} + z\,{}^0G^{PbO-L}_{PbO} + A^{Fe_xPb_zO_{3x/2+z}} + B^{Fe_xPb_zO_{3x/2+z}}T $$

where A and B are adjustable coefficients to be calculated for each oxide. The other phases are described by the compound energy model applied to oxide system [22]. Only one temperature-dependant B coefficient cannot describe reasonably the heat capacity evolution of the compound.

4.2.2. $-Fe_2O_3$ end compound

To ensure the compatibility with other Fe–M–O assessments, the model used in previous assessments for this phase is kept [23]. The model is then represented by the formula $(Fe^{3+})_2(O^{2-})_3$. The

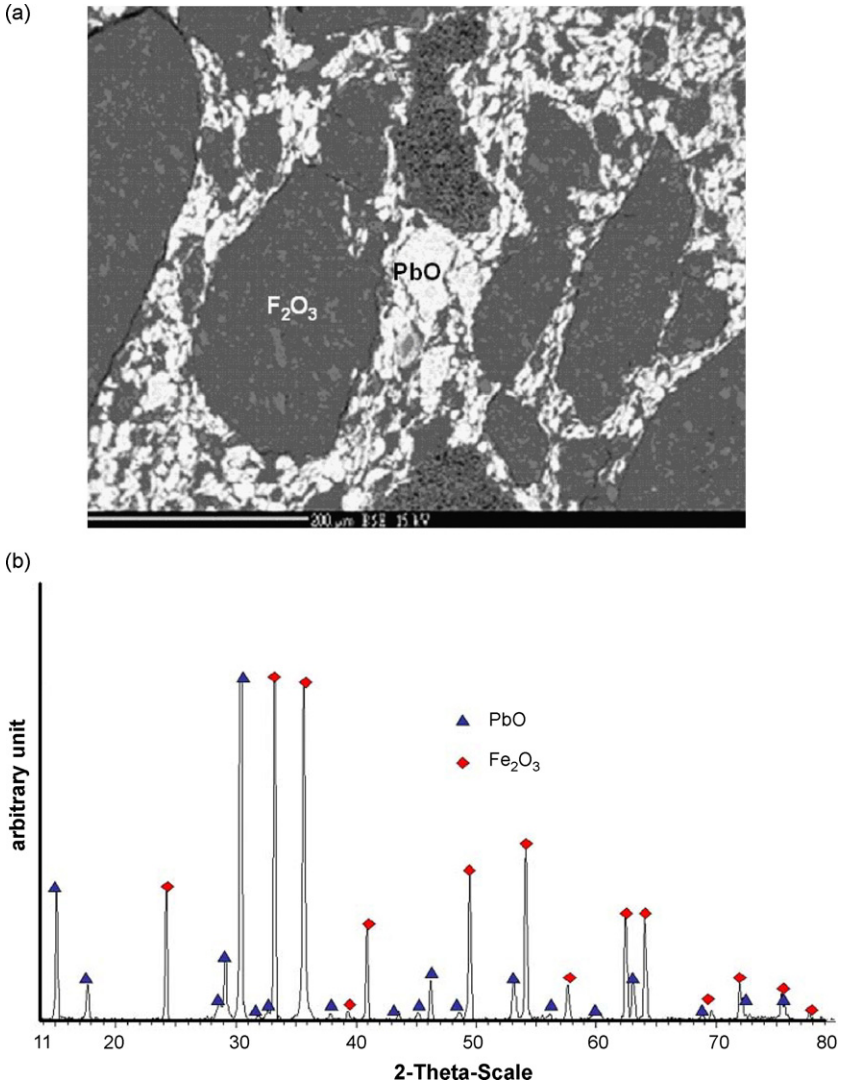

Fig. 4. SEM micrograph (*a*) and XRD (*b*) of mixture PbO–Fe_2O_3 (55 mol.% Fe_2O_3) (T = 600 °C, PO_2 = 0.21 atm, t = one month).

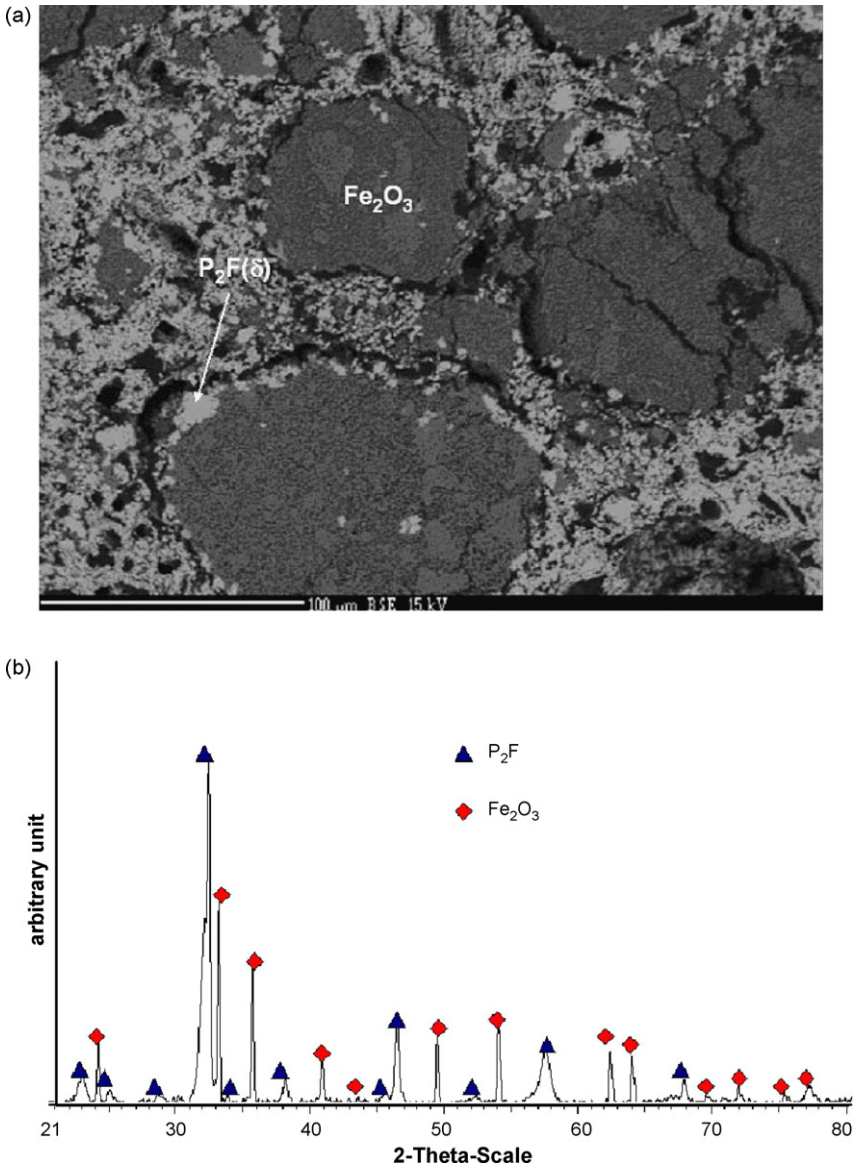

Fig. 5. SEM micrograph (a) and XRD (b) of mixture PbO–Fe_2O_3 (68 mol.% Fe_2O_3) (T = 713 °C, PO_2 = 0.21 atm, t = one month).

molar Gibbs energy of the Fe_2O_3 phase is given by

$$G_m^{Fe_2O_3} = {}^0G^{Fe_2O_3}_{Fe^{3+}:O^{2-}} + RT(x_{Fe^{3+}} \ln x_{Fe^{3+}} + x_{O^{-2}} \ln x_{O^{2-}})$$

The magnetic contribution to the Gibbs energy is described as in [23,24]. The ${}^0G^{Fe_2O_3}_{Fe^{3+}:O^{2-}}$ term is taken from previous evaluation [23].

4.2.3. –PbO-L and PbO-M end compounds

The two PbO phases (Litharge, tP4, low temperature form; Massicot, oP8, high temperature form) have only two crystallographic sites, one for Pb atoms and one for oxygen atoms. Almost authors have not put in evidence a solubility of Fe_2O_3 in PbO phases except Shaaban et al. [13]. However, a solubility of Bi_2O_3 in PbO is observed in the Bi_2O_3–PbO system. In order to describe this solubility and that of Fe_2O_3 in PbO by the same phase description, it seems reasonably to envisage that Bi^{3+} and Fe^{3+} substitutes randomly for Pb^{2+} and extra vacancies are created on the oxygen sublattice to compensate for the valence of the cations. For the present study, the model is then represented by the formula $(Fe^{3+}, Pb^{2+})_1(O^{2-}, Va)_2$. Descriptions of the two phases being the same, L or M letters are not written in the Gibbs energy equations. The only difference in the two descriptions is the ${}^0G^{PbO}_{PbO}$ reference term which is equal to ${}^0G^{PbO\text{-}L}_{PbO}$ and ${}^0G^{PbO\text{-}M}_{PbO}$ for PbO-L and PbO-M respectively (see Tables 3a and 3b). The molar Gibbs energy of the phase is given by

$$\begin{aligned} G_m^{PbO} = {} & y_{Fe^{3+}} y_{O^{2-}} {}^0G^{PbO}_{Fe^{3+}:O^{2-}} \\ & + y_{Pb^{2+}} y_{O^{2-}} {}^0G^{PbO}_{Pb^{2+}:O^{2-}} + y_{Fe^{3+}} y_{Va} {}^0G^{PbO}_{Fe^{3+}:Va} + y_{Pb^{2+}} y_{Va} {}^0G^{PbO}_{Pb^{2+}:Va} \\ & + RT(y_{Fe^{3+}} \ln y_{Fe^{3+}} + y_{Pb^{2+}} \ln y_{Pb^{2+}}) \\ & + 2RT(y_{O^{2-}} \ln y_{O^{2-}} + y_{Va} \ln y_{Va}) + {}^{Ex}G_m^{PbO} \end{aligned}$$

The Gibbs energy of the two neutral end compounds Fe_2O_3 and PbO are given by

$${}^0G^{PbO}_{Fe_2O_3} = \frac{3}{2} {}^0G^{PbO}_{Fe^{3+}:O^{2-}} + \frac{1}{2} {}^0G^{PbO}_{Fe^{+3}:Va} + 2RT\left(\frac{3}{2}\ln\frac{3}{2} + \frac{1}{2}\ln\frac{1}{2}\right)$$

and

$$G^{PbO}_{PbO} = \frac{1}{2} {}^0G^{PbO}_{Pb^{2+}:O^{2-}} + \frac{1}{2} {}^0G^{PbO}_{Pb^{2+}:Va} + 2RT\left(\frac{1}{2}\ln\frac{1}{2} + \frac{1}{2}\ln\frac{1}{2}\right)$$

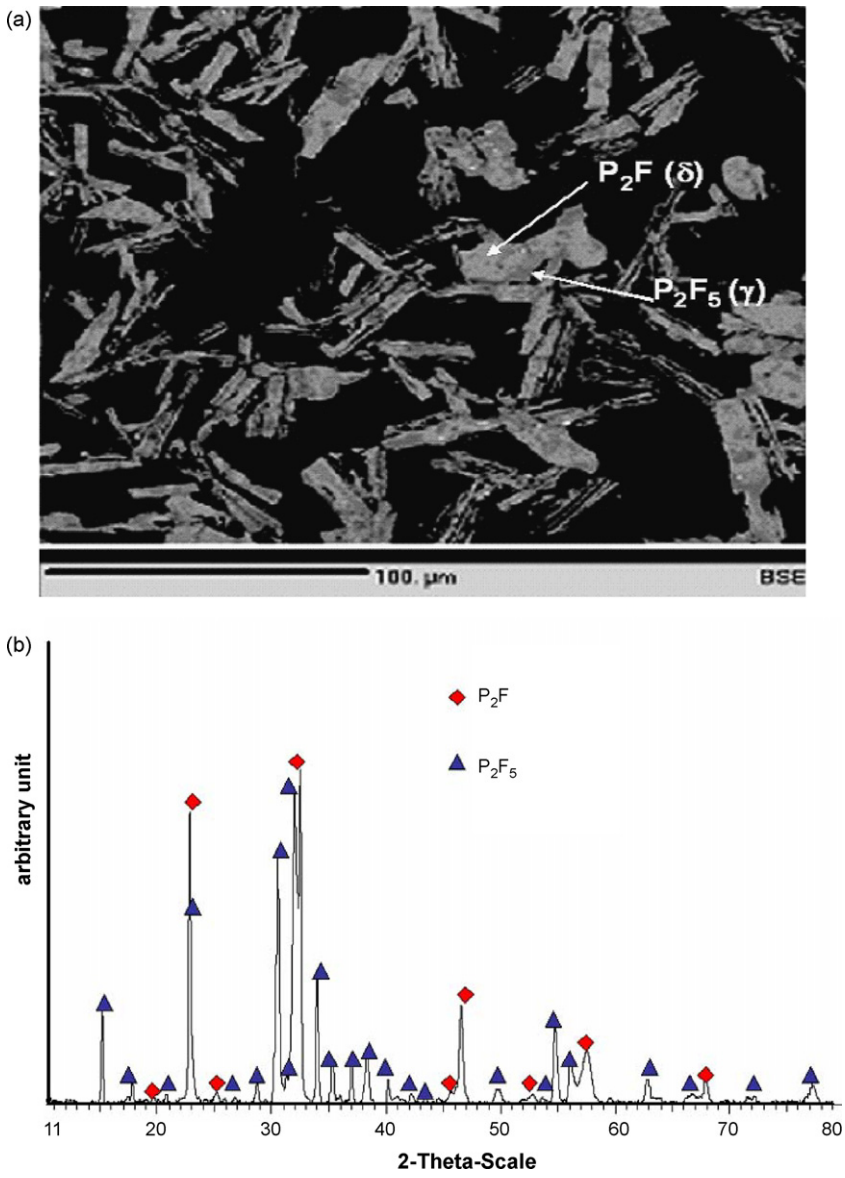

Fig. 6. SEM micrograph (a) and XRD (b) of mixture PbO–Fe_2O_3 (55 mol.% Fe_2O_3) (T = 800 °C, PO_2 = 0.21 atm, t = 2 h).

${}^{0}G^{PbO}_{Pb^{2+}:Va}$ is chosen as reference and has the value

$$ {}^{0}G^{PbO}_{Pb^{2+}:Va} = {}^{0}G^{PbO}_{PbO} - \frac{1}{2}{}^{0}G^{Gas}_{O_2} + 2RT\left(\frac{1}{2}\ln\frac{1}{2} + \frac{1}{2}\ln\frac{1}{2}\right) $$

The other terms are

$$ {}^{0}G^{PbO}_{Fe^{3+}:O^{2-}} = \frac{1}{2}{}^{0}G^{Fe_2O_3}_{Fe_2O_3} + \frac{1}{4}{}^{0}G^{Gas}_{O_2} - 2RT\left(\frac{3}{4}\ln\frac{3}{4} + \frac{1}{4}\ln\frac{1}{4}\right) + A^{PbO} + B^{PbO}T $$

$$ {}^{0}G^{PbO}_{Fe^{3+}:Va} = \frac{1}{2}{}^{0}G^{Fe_2O_3}_{Fe_2O_3} - \frac{3}{4}{}^{0}G^{Gas}_{O_2} - 2RT\left(\frac{3}{4}\ln\frac{3}{4} + \frac{1}{4}\ln\frac{1}{4}\right) + A^{PbO} + B^{PbO}T $$

$$ {}^{0}G^{PbO}_{Pb^{2+}:O^{2-}} = {}^{0}G^{PbO}_{PbO} + \frac{1}{2}{}^{0}G^{Gas}_{O_2} + 2RT\left(\frac{1}{2}\ln\frac{1}{2} + \frac{1}{2}\ln\frac{1}{2}\right) $$

No ${}^{Ex}G^{PbO}_{m}$ molar excess Gibbs energy is optimized in this work.

4.3. Ionic liquid phase

The liquid phase is described by the mean of the Hillert's partially ionic liquid model [21]. This model of the liquid phase is inspired by the concept due to Temkin [20] who had proposed a description of a crystal solid composed by two sublattices, one for cations and second one for anions. Hillert et al. [21] have developed this model which can be consider as one of the most appropriated descriptions for liquid phase in the case of oxide systems. The two-sublattice model for ionic liquids provides a continuous description from a metal liquid to an oxide liquid [21,25]. For example, this model has been used by Risold et al. for the assessment of the ionic liquid phase of the Pb–O system [26] and by Sundman [23] and Selleby and Sundman [27] for the assessment of the ionic liquid phase of the Fe–O system.

For the present work the ionic liquid phase is modeled assuming divalent iron and lead ions on the cation "sublattice" and divalent oxygen ions and vacancies (Va, having charge $-Q$) on the anion "sublattice". An associated specie $FeO_{1.5}$ is also introduced on the anion sublattice as suggested by [27]. The general occupancy of the two "sublattices" can be written as $(Fe^{2+}, Pb^{2+})_P\,(O^{2-},$

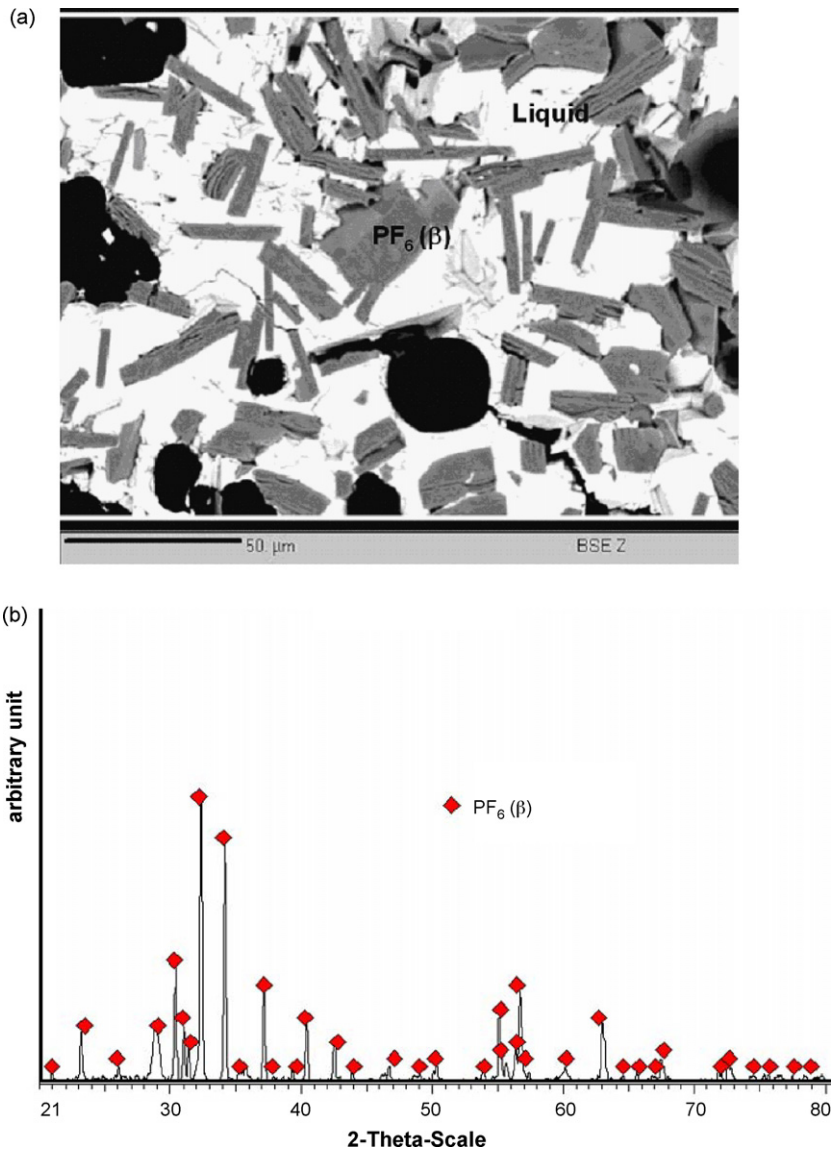

Fig. 7. SEM micrograph (a) and XRD (b) of mixture PbO–Fe_2O_3 (40 mol.% Fe_2O_3) (T = 920 °C, PO_2 = 0.21 atm, t = 2 h).

$Va^{Q-}, FeO_{1.5})_Q$. where P and Q are the site numbers of each sublattice in the ionic liquid model. The stoichiometric factors P and Q vary with the composition in order to maintain electroneutrality. Hypothetical vacancies with an induced charge are introduced in the second sublattice to make the model continuous to the metal liquid.

$$P = \sum_i y_i(-v_i) + y_{Va}(-Q)$$

$$Q = \sum_j y_j(v_j)$$

where v_i is the valence of ion i and y_i is the site fraction. The summation over i is made for all anions, and the summation over j is made for all cations.

The model assumes that the vacancies have an induced charge equal to the average charge on the cation sublattice, which is equal to Q. In the case of PbO–Fe_2O_3, $Q = 2y_{Fe^{2+}} + 2y_{Pb^{2+}}$ and $P = 2y_{O^{2-}} + Qy_{V^{Q-}}$.

The molar Gibbs energy of the liquid is:

$$\begin{aligned}
G_m^{\text{Ionic}} &= y_{Fe^{2+}}y_{O^{2-}}{}^0G^{\text{Ionic}}_{Fe^{2+}:O^{2-}} + y_{Pb^{+2}}y_{O^{2-}}{}^0G^{\text{Ionic}}_{Pb^{2+}:O^{2-}} \\
&+ Q(y_{Fe^{2+}}y_{Va}{}^0G^{\text{Ionic}}_{Fe^{2+}:Va} + y_{Pb^{2+}}y_{Va}{}^0G^{\text{Ionic}}_{Pb^{+2}:Va}) + Qy_{FeO_{1.5}}{}^0G^{\text{Ionic}}_{FeO_{1.5}} \\
&+ PRT(y_{Fe^{2+}}\ln y_{Fe^{2+}} + y_{Pb^{2+}}\ln y_{Pb^{2+}}) \\
&+ QRT(y_{O^{2-}}\ln y_{O^{2-}} + y_{Va}\ln y_{Va} + y_{FeO_{1.5}}\ln y_{FeO_{1.5}}) + {}^{Ex}G_m^{\text{Ionic}} \\
{}^{Ex}G_m^{\text{Ionic}} &= y_{Fe^{2+}}y_{O^{2-}}y_{Va}\sum L^{\upsilon,\text{Ionic}}_{Fe^{2+}:O^{2-},Va}(y_{O^{2-}} - y_{Va})^{\upsilon} \\
&+ y_{Pb^{2+}}y_{O^{2-}}y_{Va}\sum L^{\upsilon,\text{Ionic}}_{Pb^{2+}:O^{2-},Va}(y_{O^{2-}} - y_{Va})^{\upsilon} \\
&+ y_{Fe^{2+}}y_{Pb^{2+}}y_{O^{2-}}L^{0,\text{Ionic}}_{Fe^{2+},Pb^{2+}:O^{2-}} + y_{Fe^{2+}}y_{Pb^{2+}}y_{Va}L^{0,\text{Ionic}}_{Fe^{2+},Pb^{2+}:Va} \\
&+ y_{Fe^{2+}}y_{O^{2-}}y_{FeO_{1.5}}\sum L^{\upsilon,\text{Ionic}}_{Fe^{2+}:O^{2-},FeO_{1.5}}(y_{O^{2-}} - y_{FeO_{1.5}})^{\upsilon} \\
&+ y_{Pb^{2+}}y_{O^{2-}}y_{FeO_{1.5}}L^{0,\text{Ionic}}_{Pb^{2+}:O^{2-},FeO_{1.5}} \\
&+ y_{Fe^{2+}}y_{Va}y_{FeO_{1.5}}L^{0,\text{Ionic}}_{Fe^{2+}:Va,FeO_{1.5}} + y_{Pb^{2+}}y_{Va}y_{FeO_{1.5}}L^{0,\text{Ionic}}_{Pb^{2+}:Va,FeO_{1.5}}
\end{aligned}$$

$L^{\upsilon,\text{Ionic}}_{Fe^{2+}:O^{2-},Va}$, $L^{\upsilon,\text{Ionic}}_{Pb^{2+}:O^{2-},Va}$, $L^{\upsilon,\text{Ionic}}_{Fe^{2+}:O^{2-},FeO_{1.5}}$, and $L^{0,\text{Ionic}}_{Fe^{2+}:Va,FeO_{1.5}}$ represent interactions in the binary Pb–O and Fe–O systems and are taken from [23,26,27]. $L^{0,\text{Ionic}}_{Fe^{2+},Pb^{2+}:Va}$ parameter represents inter-

actions between metallic elements. $L^{0,\text{Ionic}}_{Fe^{2+},Pb^{2+}:O^{2-}}$ represents an interaction term between the two cations in the presence of the anion. $L^{0,\text{Ionic}}_{Pb^{+2}:O^{-2},FeO_{1.5}}$ and $L^{0,\text{Ionic}}_{Pb^{2+}:Va,FeO_{1.5}}$ represent interactions between Pb + 2 and a neutral. These last four interaction parameters are optimized in this work.

5. Results

5.1. Phase equilibria

The analyses of the chemical compositions of the samples have allowed concluding to the non-stoichiometry of the compound γ-$Pb_2Fe_{10}O_{17}$(2:5) and conversely to the stoichiometry of δ-$Pb_2Fe_2O_5$(2:1) and β-$PbFe_{12}O_{19}$(1:6). The limit compositions (Table 4) do not correspond exactly to those announced in the literature.

A thermogram obtained for an alloy containing 27.5 mol.% of Fe_2O_3 is given as an example (Fig. 3-a). For some alloys it has been necessary to draw the derived curve in order to determine more precisely the invariant temperatures (Fig. 3-b). In this example the temperatures of reaction are placed at 775 °C, 856 °C and 910 °C. The results obtained from DTA experiments and annealings have shown that six invariant equilibria are clearly well defined. The DTA results are reported in Tables 3a and 3b and the comparison with literature in Table 4. For each experimental reaction, an average measured temperature is given. Concerning the DTA experiments at low temperature *i.e.* performed in the temperature range 300 and 500 °C, no significant calorimetric signal is detected. This is coherent with the isothermal annealings: no intermediate compound is formed between PbO and Fe_2O_3 in this range of temperature. The analyses by EMPA and DRX have shown biphasic equilibrium PbO + Fe_2O_3 with no solubility (Fig. 4). These results are in agreement with

Table 5
Assessed parameters for the PbO–Fe_2O_3 system. The temperature range is $298.15 \le T \le 6000$. Parameters which are not listed are equal to zero.

Phase	Parameter values (J/mol of atoms)	Reference
IONIC_LIQ $(Fe^{2+}, Pb^{2+})_P(O^{2-}, Va^{Q-}, FeO_{1.5})_Q$	${}^0G^{\text{IONIC\_LIQ}}_{Fe^{2+}:Va} = +\text{GFELIQ}$	[27]
	${}^0G^{\text{IONIC\_LIQ}}_{Fe^{2+}:O^{2-}} = +4\ \text{GFEOLIQ}$	[27]
	${}^0G^{\text{IONIC\_LIQ}}_{FeO_{1.5}} = -89{,}819 + 39.962\,T + 2.5\ \text{GFEOLIQ}$	[27]
	${}^0G^{\text{IONIC\_LIQ}}_{Pb^{2+}:Va} = +\text{GPBLIQ}$	[18]
	${}^0G^{\text{IONIC\_LIQ}}_{Pb^{2+}:O^{2-}} = 2\text{GPBOLIQ}$	[26]
	$L^{0,\text{IONIC\_LIQ}}_{Fe^{2+}:Va,FeO_{1.5}} = +110{,}000$	[27]
	$L^{0,\text{IONIC\_LIQ}}_{Fe^{2+}:O^{2-},FeO_{1.5}} = -26{,}362$	[27]
	$L^{1,\text{IONIC\_LIQ}}_{Fe^{2+}:O^{2-},FeO_{1.5}} = +13{,}353$	[27]
	$L^{0,\text{IONIC\_LIQ}}_{Fe^{2+}:O^{2-},Va} = +176{,}681 - 16.368\,T$	[27]
	$L^{1,\text{IONIC\_LIQ}}_{Fe^{2+}:O^{2-},Va} = -65{,}655 + 30.869\,T$	[27]
	$L^{0,\text{IONIC\_LIQ}}_{Pb^{2+}:O^{2-},Va} = +168{,}750 - 61\,T$	[26]
	$L^{1,\text{IONIC\_LIQ}}_{Pb^{2+}:O^{2-},Va} = +29{,}510 - 20\,T$	[26]
	$L^{0,\text{IONIC\_LIQ}}_{Pb^{2+}:O^{2-},FeO_{1.5}} = -10{,}638$	This work
Fe_2O_3 $(Fe^{3+})_2$ $(O^{2-})_3$	${}^0G^{Fe_2O_3}_{Fe^{3+}:O^{2-}} = +GFE2O3$	[27]
	${}^0TC^{Fe_2O_3}_{Fe^{3+}:O^{2-}} = -2867$	[27]
	${}^0\beta^{Fe_2O_3}_{Fe^{3+}:O^{2-}} = -25.1$	[27]
δ-$Pb_2Fe_2O_5$(2:1)	${}^0G^{Pb_2FeO_5}_{Pb^{2+}:Fe^{3+}:O^{2-}} = +39{,}813 - 42.22\,T + 2\,GPBOL + GFE2O3$	This work
γ-$Pb_2Fe_{10}O_{17}$(2:5)	${}^0G^{Pb_2Fe_{10}O_{17}}_{Pb^{2+}:Fe^{3+}:O^{2-}} = +59{,}484 - 60.90\,T + 2\,GPBOL + 5\,GFE2O3$	This work
β-$PbFe_{12}O_{19}$(1:6)	${}^0G^{PbFe_{12}O_{19}}_{Pb^{2+}:Fe^{3+}:O^{2-}} = +40{,}406 - 40.39\,T + GPBOL + 6\,GFE2O3$	This work
PbOL $(Fe^{3+}, Pb^{2+})_1(O^{2-}, Va)_2$	${}^0G^{\text{PbO-L}}_{Fe^{3+}:O^{2-}} = +0.5\,GFE2O3 + 0.25\,GO2GAS - 2\,RT\left(\frac{3}{4}\ln\frac{3}{4} + \frac{1}{4}\ln\frac{1}{4}\right) + 100{,}000$	This work
	${}^0G^{\text{PbOL}}_{Fe^{3+}:Va} = +0.5\,GFE2O3 - 0.75\,GO2GAS - 2\,RT\left(\frac{3}{4}\ln\frac{3}{4} + \frac{1}{4}\ln\frac{1}{4}\right) + 100{,}000$	This work
	${}^0G^{\text{PbOL}}_{Pb^{2+}:O^{2-}} = +GPBOL + 0.5\,GO2GAS + 2\,RT\ln 2$	This work
	${}^0G^{\text{PbOL}}_{Pb^{2+}:Va} = +GPBOL - 0.5\,GO2GAS + 2\,RT\ln 2$	This work
PbOM $(Fe^{2+}, Pb^{2+})_1(O^{2-}, Va)_2$	${}^0G^{\text{PbOM}}_{Fe^{3+}:O^{2-}} = +0.5\,GFE2O3 + 0.25\,GO2GAS - 2\,RT\left(\frac{3}{4}\ln\frac{3}{4} + \frac{1}{4}\ln\frac{1}{4}\right) + 100{,}000$	This work
	${}^0G^{\text{PbOM}}_{Fe^{3+}:Va} = +0.5\,GFE2O3 - 0.75\,GO2GAS - 2\,RT\left(\frac{3}{4}\ln\frac{3}{4} + \frac{1}{4}\ln\frac{1}{4}\right) + 100{,}000$	This work
	${}^0G^{\text{PbOM}}_{Pb^{2+}:O^{2-}} = +GPBOM + 0.5\,GO2GAS + 2\,RT\ln 2$	This work
	${}^0G^{\text{PbOM}}_{Pb^{2+}:Va} = +GPBOM - 0.5\,GO2GAS + 2\,RT\ln 2$	This work

Definitions of the functions:

GFELIQ	$298.15 < T < 1811$	$+12{,}040.17 - 6.55843\,T - 3.6751551 \times 10^{-21}\,T^7 + GHSERFE$
	$1811 < T < 6000$	$-10{,}839.7 + 291.302\,T - 4\,T\ln(T)$
GFEOLIQ	$298.15 < T < 6000$	$-137{,}252 + 224.641\,T - 37.1815\,T\ln(T)$
GFE2O3	$298.15 < T < 6000$	$-858{,}683 + 827.946\,T - 137.0089\,T\ln(T) + 1{,}453{,}810\,T^{-1}$
GPBO	$298.15 < T < 762$	$-235{,}043 + 250.4\,T - 46.2\,T\ln(T) - 0.008\,T^2 + 225{,}000\,T^{-1}$
	$762 < T < 1160$	$-232{,}910 + 244.7\,T - 45.9\,T\ln(T) - 0.0067\,T^2 + 178{,}000\,T^{-1}$
GPBLIQ	$298.15 < T < 606.650$	$+4672.157 - 7.750257\,T - 6.0144 \times 10^{-19}\,T^7 + GHSERPB$
	$606.650 < T < 5000$	$+4853.112 - 8.066587\,T - 8.05644 \times 10^{25}\,T^{-9} + GHSERPB$
GPBOLIQ	$298.15 < T < 6000$	$-219{,}210 + 360\,T - 65\,T\ln(T)$

Table 6
Characteristics of invariant equilibria (composition, temperature) compared with data retrieved from literature.

Invariant	Composition of phases (mol.% Fe_2O_3)						T (°C)			
	Experimental			Calculated			Calculated	[8]	[14]	[15]
L + Fe_2O_3 → (1:6)	–	–	–	41.4	100	85.7	1301	1315	1315	1300
L + (1:6) → (2:5)	20.3	84.5	74.8	20.1	85.7	71.4	915	945	880	915
L + (2:5) → (2:1)	17.7	74.6	32.5	18.4	71.4	33.3	870	910	870	870
(1:6) → (2:5) + Fe_2O_3	–	–	–	85.7	71.4	100	800	760	–	–
(2:5) → (2:1) + Fe_2O_3	74.8	31.5	100	71.4	33.3	100	780	750	750	–
L → PbO-M + (2:1)	12.8	0	32.5	12.9	0	33.3	774	730	760	780
(2:1) → PbO-M + Fe_2O_3	33.7	0	100	33.3	0	100	680	–	–	–
PbO-M → PbO-L	0	0	0	0	762	–	–	–		

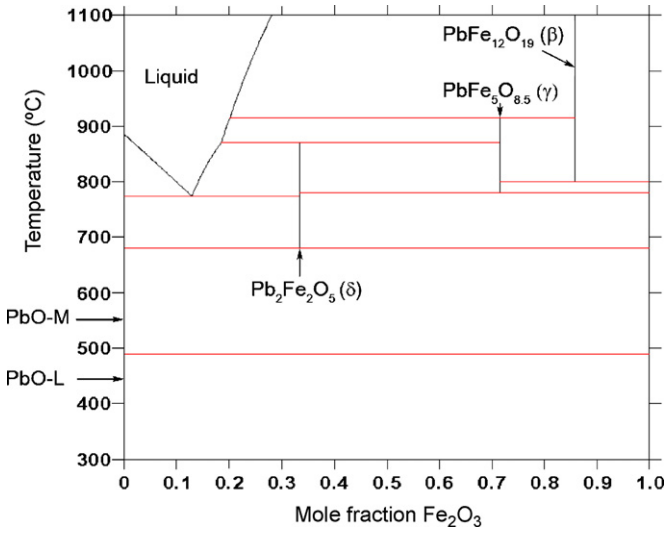

Fig. 8. Calculated PbO–Fe_2O_3 phase diagram.

literature [8,14,15]. The lower temperature invariant occurs at 710 ± 5 °C which corresponds to the eutectoïd reaction according to δ-$Pb_2Fe_2O_5$(2:1) → PbO + Fe_2O_3 (Fig. 5). The eutectic temperature is found to be equal to 775 ± 5 °C. The eutectoïd temperature of decomposition of the γ-$Pb_2Fe_{10}O_{17}$(2:5) phase is very close to the previous eutectic temperature: it is equal to 778 ± 5 °C (Fig. 6). The two peritectic temperatures of the L + γ-$Pb_2Fe_{10}O_{17}$(2:5) → δ-$Pb_2Fe_2O_5$(2:1) and the L + β-$PbFe_{12}O_{19}$(1:6) → γ-$Pb_2Fe_{10}O_{17}$(2:5) reactions are 856 ± 4 °C and 910 ± 5 °C (Figs. 3 and 7) respectively which are very close to the values reported in the works performed by Nevriva and Fischer [14] and Rivolier et al. [15]. The invariant equilibria between β-$PbFe_{12}O_{19}$(1:6), γ-$Pb_2Fe_{10}O_{17}$(2:5) and Fe_2O_3 which is between 780 and 810 °C has not been measured exactly by DTA. In order to determine the nature of this reaction several isothermal annealings are performed between 600 and 800 °C on a sample containing 90 mol.% of Fe_2O_3. Then, the samples are analysed by DRX. These analyses have shown the appearance of β-$PbFe_{12}O_{19}$(1:6) phase at 770 °C (peritectoid reaction γ-$Pb_2Fe_{10}O_{17}$(2:5) + Fe_2O_3 → β-$PbFe_{12}O_{19}$(1:6)). The highest temperature of peritectic reactions observed by some authors is measured with a poor reproducibility (1302 ± 45 °C) which probably depends on the instability of Fe_2O_3 above 1290 °C. This is in agreement with the work of Rivolier et al. [15].

5.2. Modeling

A thermodynamic description of the low temperature part of the pseudo-binary PbO–Fe_2O_3 system is performed according to the Calphad approach. It has allowed taking into account almost of the available data issued from Mountvala and Ravitz [8], Nevriva and Fischer [14] and Rivolier et al. [15]. The δ-$Pb_2Fe_2O_5$(2:1) and β-$PbFe_{12}O_{19}$(1:6) phases are considered as stoichiometric compounds as required by literature. In order to simply the description of the system, the same model is applied to describe γ phase although EPMA analyses have put in evidence a non-homogeneity range. The retained stoichiometry for is γ-$Pb_2Fe_{10}O_{17}$(2:5). It is important to notice that according to the knowledge of the authors, any specific thermodynamic property has not been measured on this system: neither enthalpy of formation/mixing or specific heat by calorimetry nor chemical potential by electromotive forces technique. This lack of thermodynamic data conducts to an imperfect description. Moreover the existence of equilibria with phases being outside of the cut prevents a relevant modeling of its thermodynamic description. The assessment of model parameters for the ionic liquid phase and for solid phases is performed using the optimisation software "PARROT" developed by Jansson [28] and included in the Thermo-Calc software [29]. For the Fe_2O_3-rich endpoint, temperature-independent parameters are optimized for PbO-L and PbO-M phases. The description of PbO-L and PbO-M being equivalent $A^{\text{PbO-L}}$ and $A^{\text{PbO-M}}$ are equal. For the PbO-rich endpoint, no parameter is used for Fe_2O_3 phase. For the three stoichiometric phases $A^{Bi_xPb_zO_{3x/2+z}}$ and $B^{Bi_xPb_zO_{3x/2+z}}$ terms are optimized. Concerning the liquid phase, only a temperature-independent regular interaction parameter is optimized ($L^{0,\text{IONIC\_LIQ}}_{Pb^{2+}:O^{2-},FeO_{1.5}}$). Table 5 give the thermodynamic set of parameters. The resulting phase diagram is presented in Fig. 8 and is in well agreement with all experimental points retrieved from literature. Experimental invariant equilibrium temperatures are compared to those calculated on Table 6.

6. Conclusions

This work represents a contribution to the study of PbO–Fe_2O_3 system. The experimental investigations have allowed determining the existence of two mixed compounds and a γ solid solution. Low temperature mixtures between PbO and Fe_2O_3 do not conducted to the formation of intermediate phases. Moreover no solubility of PbO in Fe_2O_3 and Fe_2O_3 in PbO phases is measured at different temperatures. Considering the lack of thermodynamic data, a thermodynamic description of the system is performed conducting to a consistent set of parameters. The resulting phase diagram is in good agreement with the available compiled data.

Acknowledgments

A part of this work was financially supported by GEDEPEON (GDR). The authors wish to thank J. Ravaux, responsible of the SCMEM of the Université Henri Poincaré who carried out the SEM and microprobe analysis of the samples.

References

[1] A. Maître, M. François, R. Podor, J.C. Gachon, Mater. Sci. Forum (2004) 461.
[2] A. Maître, J.M. Fiorani, J.J. Kuntz, J.C. Gachon, J. Physique IV 12 (2002) 163.

[3] A. Maître, J.M. Fiorani, J.C. Gachon, M. Vilasi, J. Physique IV (2004) 69.
[4] A. Maître, M. François, J.C. Gachon, J. Phase Equilibr. Diffusion 25 (2004) 59.
[5] A. Cocco, Annali Chim. 45 (1955) 737.
[6] W. Berger, F. Pawlek, Arch. Eisenhuettenwesen 28 (1957) 101.
[7] E.V. Margulis, N.I. Kopylov, Zhurnal Neorganicheskoi Khimii 5 (1960) 2471.
[8] A.J. Mountvala, S.F. Ravitz, J. Am. Ceram. Soc. 45 (1962) 285.
[9] D.M. Chizhikov, T.E. Konvshkova, Akademii Nauk SSSR 12 (1963) 72.
[10] V.E. Rudnichenko, B.L. Dobrotsvetov, D.M. Kheiker, Gos. Nauchn.: Issled. Inst. Tsvetn. Metal. 23 (1965) 389.
[11] H.D. Jonker, J. Cryst. Growth 28 (1975) 231.
[12] J. Mexmain, S.L. Hivert, Annales Chim. 3 (1978) 91.
[13] S.A. Shaaban, M.F. Abadir, A.N. Mahdy, Trans. J. Br. Ceram. Soc. 83 (1984) 102.
[14] M. Nevriva, K. Fischer, Mater. Res. Bull. 21 (1986) 1285.
[15] J.L. Rivolier, M. Ferriol, R. Abraham, M.T. Cohen-Adad, Eur. J. Solid State Inorg. Chem. 30 (1993) 727.
[16] JCPDS – International Centre for Diffraction Data, Database, 2003.
[17] P. Kofstad, High Temperature Corrosion, Elsevier Applied Science, London/New York, 1988.
[18] A.T. Dinsdale, Calphad 15 (1991) 317.
[19] B. Sundman, J. Agren, J. Phys. Chem. Solids 42 (1981) 297.
[20] M. Temkin, Acta Phys. Chem. 20 (1945) 411.
[21] M. Hillert, B. Jansson, B. Sundman, J. Agren, Metall. Trans. A: Phys. Metall. Mater. Sci. 16A (1985) 261.
[22] M. Hillert, B. Jansson, B. Sundman, Z. Metallkunde 79 (1988) 81.
[23] B. Sundman, J. Phase Equilibr. 12 (1991) 127.
[24] G. Inden, M. Jarl, Calphad 2 (1978) 227.
[25] B. Sundman, Calphad 15 (1991) 109.
[26] D. Risold, J.I. Nagata, R.O. Suzuki, J. Phase Equilibr. 19 (1998) 213.
[27] M. Selleby, B. Sundman, Calphad 20 (1996) 381.
[28] B. Jansson, Thesis, Royal Institute of Technology, Stockholm, 1984.
[29] B. Sundman, B. Jansson, J.O. Andersson, Calphad 9 (1985) 153.